

1 Inventory of Supporting Information

2

3 **Proteomic Profiling of Cerebrospinal Fluid Identifies Immune and**

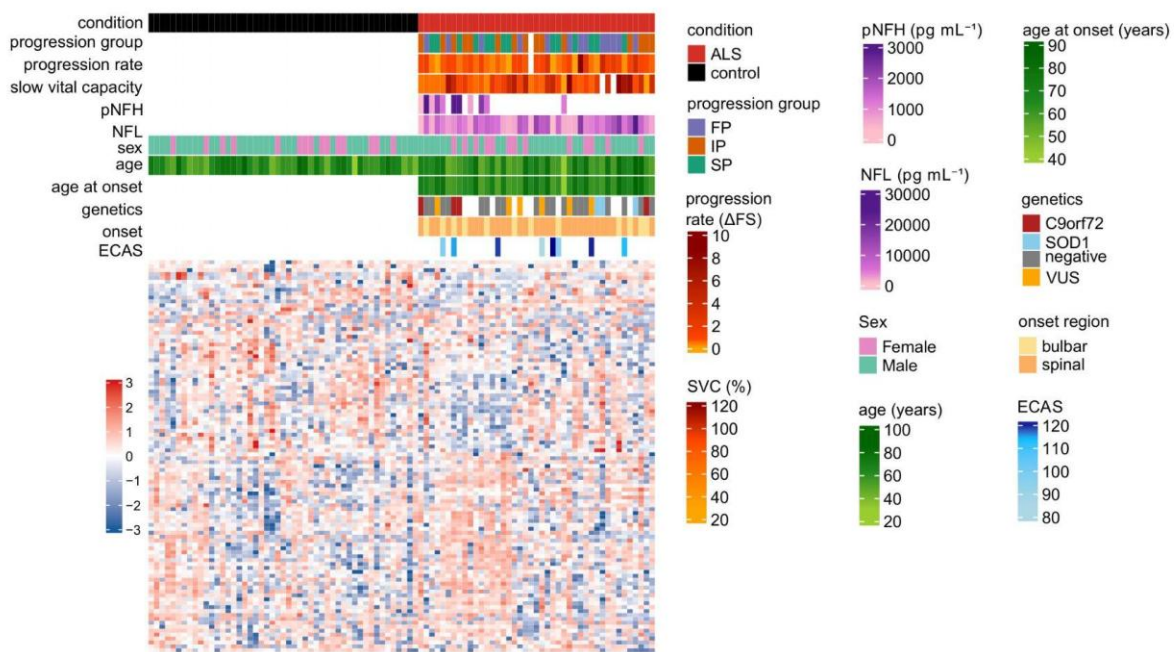
4 **Synapto-Axonal ALS Subtypes**

5 Tzeplaeff and Liu et al., 2025.

6

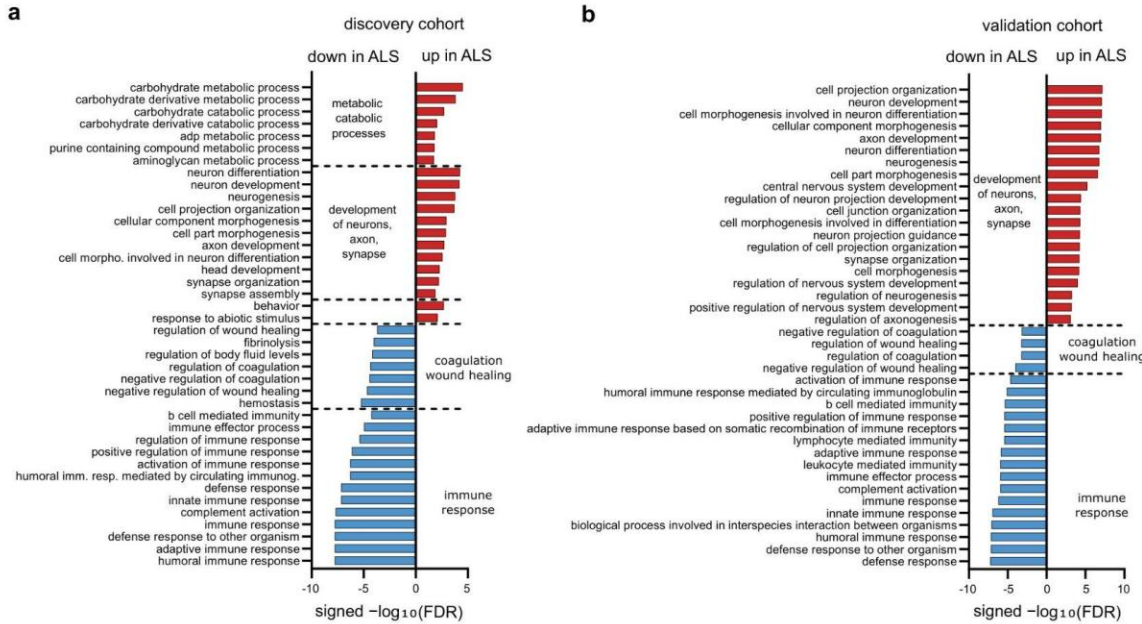
7 **List of contents**

9	Extended Data Fig. 1 Heatmap and clinical characteristics of the validation cohort ...	2
10	Extended Data Fig. 2 Gene set enrichment analysis of ALS versus control in the	
11	discovery and validation cohorts.	3
12	Extended Data Fig. 3 Concordance of GSEA pathway enrichment between the	
13	discovery and validation cohorts.	4
14	Extended Data Fig. 4 Clustering selection and visualization of proteomic subtypes ..	5
15	Extended Data Fig. 5 Gene set enrichment analysis comparing alpha and beta	
16	subtypes in the discovery and validation cohorts.	6
17	Extended Data Fig. 6 Concordance of GSEA pathway enrichment between alpha and	
18	beta subtypes in the discovery and validation cohorts.	7
19	Extended Data Fig. 7 Proteomic clustering and subtype characterization in the	
20	external cohort.	8
21	Extended Data Fig. 8 Clinical characteristics stratified by ALS alpha and beta	
22	subtypes in the discovery and validation cohorts.	9
23	Extended Data Fig. 9 Top 6 proteins of the turquoise and blue modules in the	
24	discovery cohort.	10
25	Extended Data Fig. 10 Clustering of brain proteomic samples.	11
26		



27

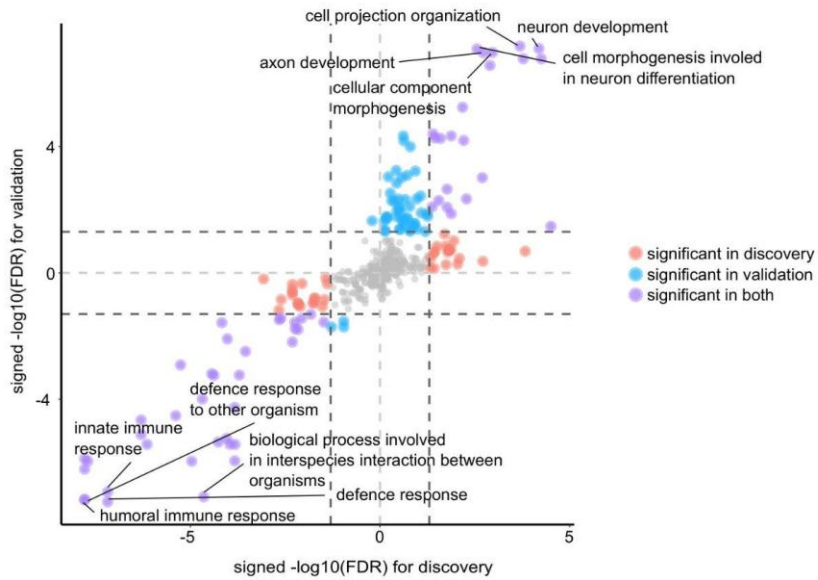
28 **Extended Data Fig. 1 | Heatmap and clinical characteristics of the validation cohort.**
29 Heatmap showing the 100 most variable cerebrospinal fluid (CSF) proteins in the validation
30 cohort. Rows represent proteins and columns represent individual samples. Demographic and
31 clinical variables are annotated, including condition, sex, age and age at onset (years), CSF
32 neurofilament light chain (NEFL) and phosphorylated neurofilament heavy chain (pNFH)
33 levels (pg mL^{-1}), slow vital capacity (SVC, %), Edinburgh Cognitive and Behavioural ALS
34 Screen (ECAS) score, site of onset, disease progression rate (Δ Functional score per month),
35 progression group, and genetic status. White indicates missing or unavailable data.



36

37 **Extended Data Fig. 2 | Gene set enrichment analysis of ALS versus control in the**
 38 **discovery and validation cohorts.**

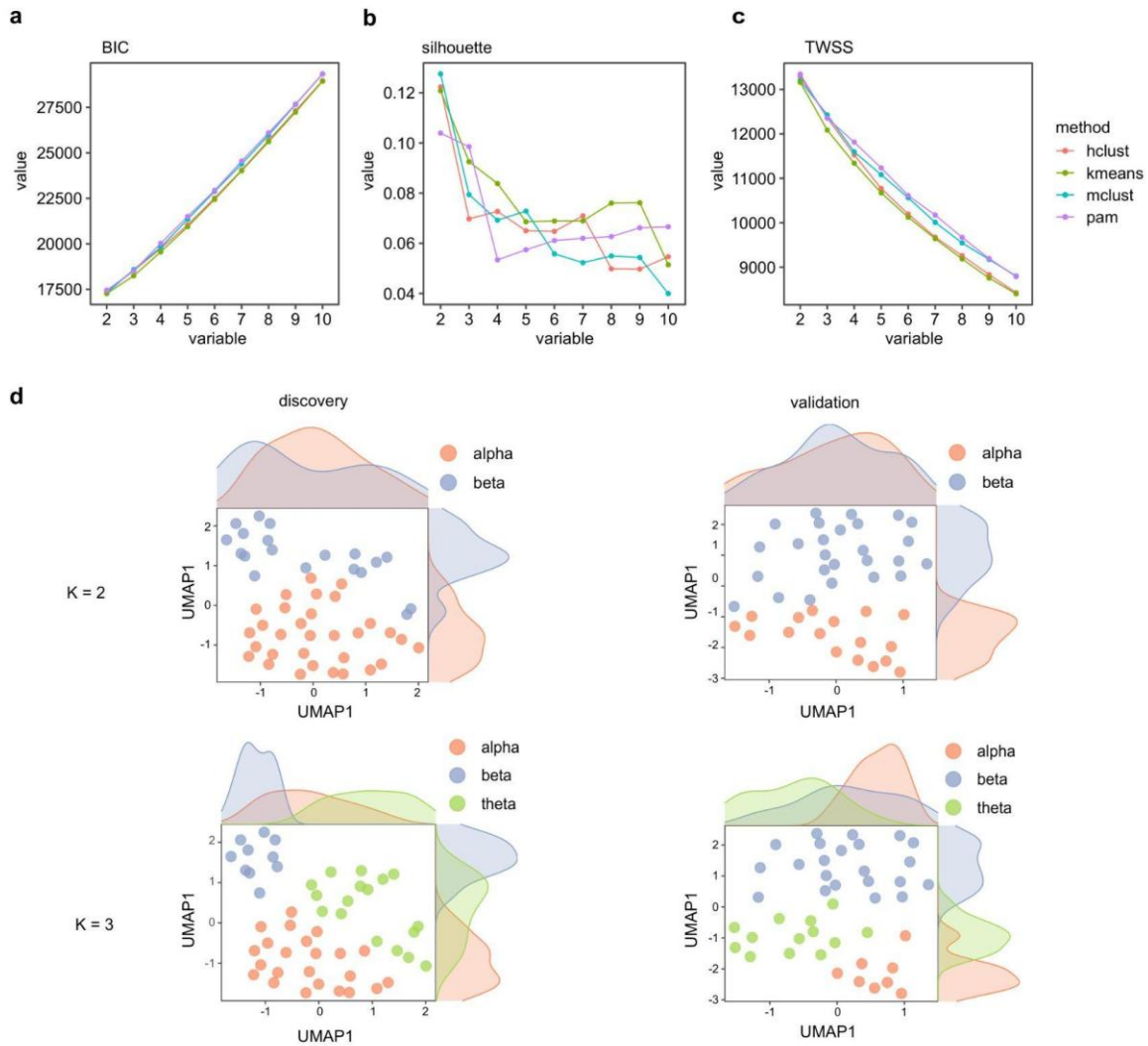
39 **a,b**, Gene set enrichment analysis (GSEA) Gene Ontology Biological Process (GO BP) terms
 40 in the discovery cohort (a) and the validation cohort (b). The top 20 significantly upregulated
 41 (red) and downregulated (blue) enriched GO BP terms ($\text{FDR} < 0.05$) in ALS versus controls
 42 are shown. Data are represented as signed $-\log_{10}(\text{FDR})$. Related GO terms were manually
 43 grouped into broader functional categories.



44

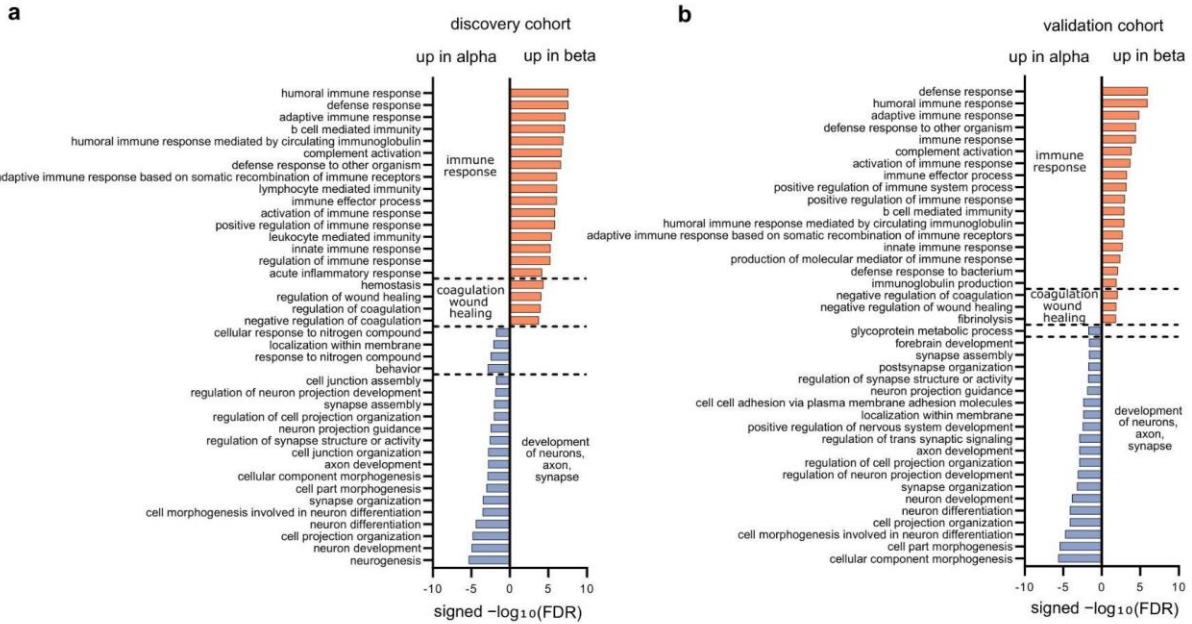
45 **Extended Data Fig. 3 | Concordance of GSEA pathway enrichment between the**
 46 **discovery and validation cohorts.**

47 Scatter plot showing the correlation of commonly enriched Gene Ontology Biological Process
 48 (GO BP) terms between the discovery and validation cohorts following comparison of ALS
 49 versus controls. Data are represented as signed $-\log_{10}(\text{FDR})$, with downregulated biological
 50 processes in ALS shown as values < 0 and upregulated processes shown as values > 0 . GO
 51 BP terms dysregulated exclusively in the discovery cohort are shown in pink, terms
 52 dysregulated exclusively in the validation cohort in blue, and terms dysregulated in both
 53 cohorts in purple. Correlation and statistical significance were assessed using Pearson's
 54 product-moment correlation ($r = 0.85$; $P < 2.2\text{e-}16$).



57 **Extended Data Fig. 4 | Clustering selection and visualization of proteomic subtypes.**

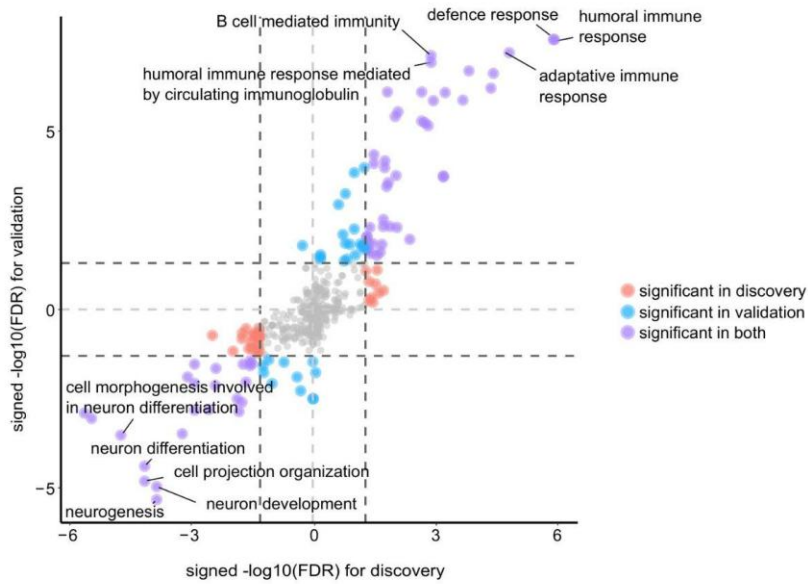
58 **a-c**, Clustering performance metrics evaluated in the discovery cohort. Bayesian Information
 59 Criterion (BIC) (a), silhouette score (b), and total within-cluster sum of squares (TWSS) (c)
 60 are shown for four clustering algorithms: hierarchical clustering (hclust), k-means clustering
 61 (k-means), model-based clustering (mclust), and partitioning around medoids (PAM). Cluster
 62 numbers ranging from two to ten ($k = 2-10$) were tested. The k-means algorithm with two to
 63 three clusters achieved an optimal balance between high silhouette scores and biological
 64 interpretability and was therefore selected as the optimal clustering approach.
 65 **d**, Uniform Manifold Approximation and Projection (UMAP) showing the distribution of
 66 proteomic samples using $k = 2$ (top panels) or $k = 3$ (bottom panels) clustering in the discovery
 67 cohort (left) and validation cohort (right). Samples are labeled according to their assignment
 68 to the alpha, beta, or theta cluster.



69

70 **Extended Data Fig. 5 | Gene set enrichment analysis comparing alpha and beta**
71 **subtypes in the discovery and validation cohorts.**

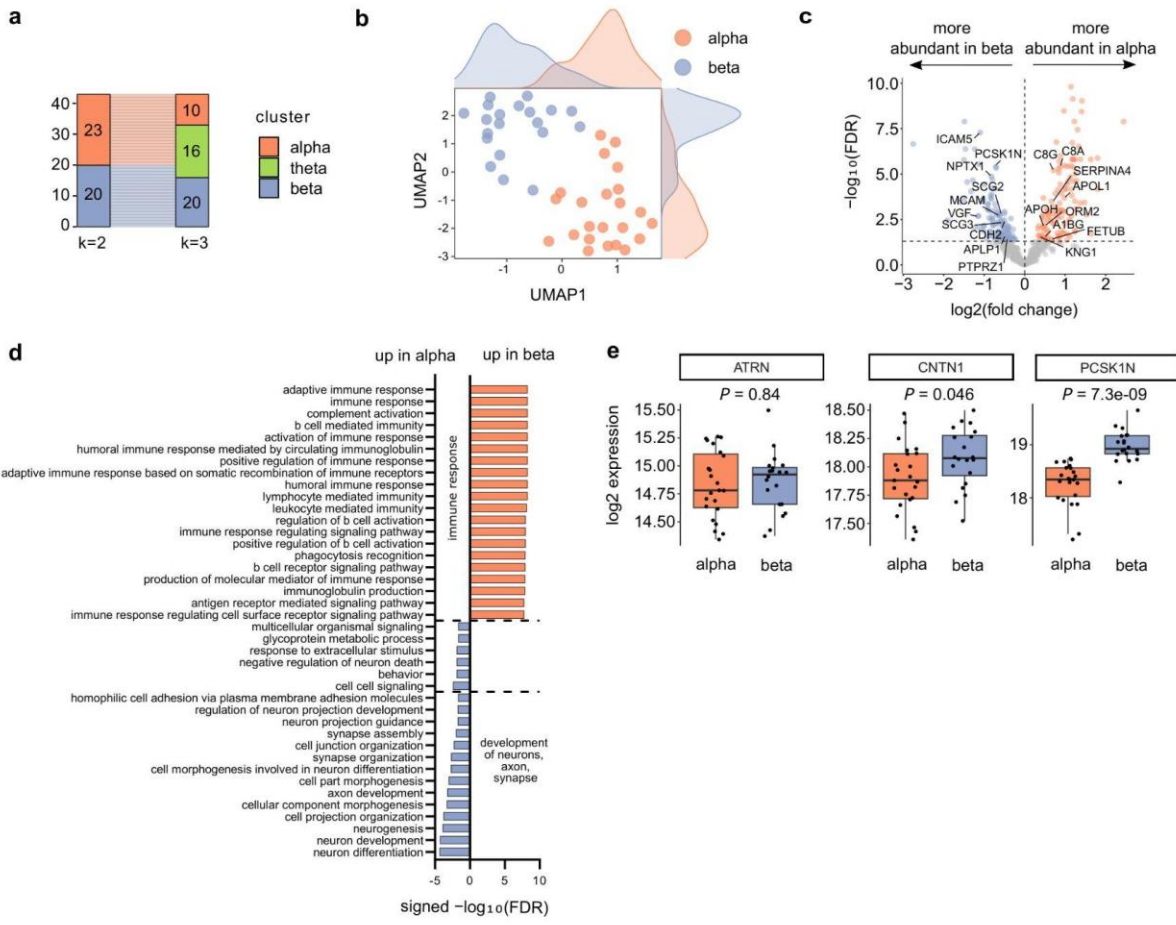
72 **a,b**, Gene set enrichment analysis (GSEA) of Gene Ontology Biological Process (GO BP)
73 terms identifying the top 20 significantly enriched pathways ($\text{FDR} < 0.05$) distinguishing the
74 alpha and beta clusters in the discovery cohort **(a)** and validation cohort **(b)**. GO BP terms
75 more enriched in the beta cluster are shown in blue, whereas those more enriched in the alpha
76 cluster are shown in orange. Data are represented as signed $-\log_{10}(\text{FDR})$. Related GO terms
77 were manually grouped into broader functional categories.



78

79 **Extended Data Fig. 6 | Concordance of GSEA pathway enrichment between alpha and**
 80 **beta subtypes in the discovery and validation cohorts.**

81 Scatter plot showing the correlation of commonly enriched Gene Ontology Biological Process
 82 (GO BP) terms between the discovery and validation cohorts following comparison of alpha
 83 versus beta subtypes. Data are represented as signed $-\log_{10}(\text{FDR})$, with GO BP terms more
 84 enriched in the beta cluster shown as values < 0 and those more enriched in the alpha cluster
 85 shown as values > 0 . GO BP terms dysregulated exclusively in the discovery cohort are shown
 86 in pink, those dysregulated exclusively in the validation cohort in blue, and those dysregulated
 87 in both cohorts in purple. Correlation and statistical significance were assessed using
 88 Pearson's product-moment correlation ($r = 0.85$; $P < 2.2\text{e-}16$).



89

90 **Extended Data Fig. 7 | Proteomic clustering and subtype characterization in the external**
91 **cohort.**

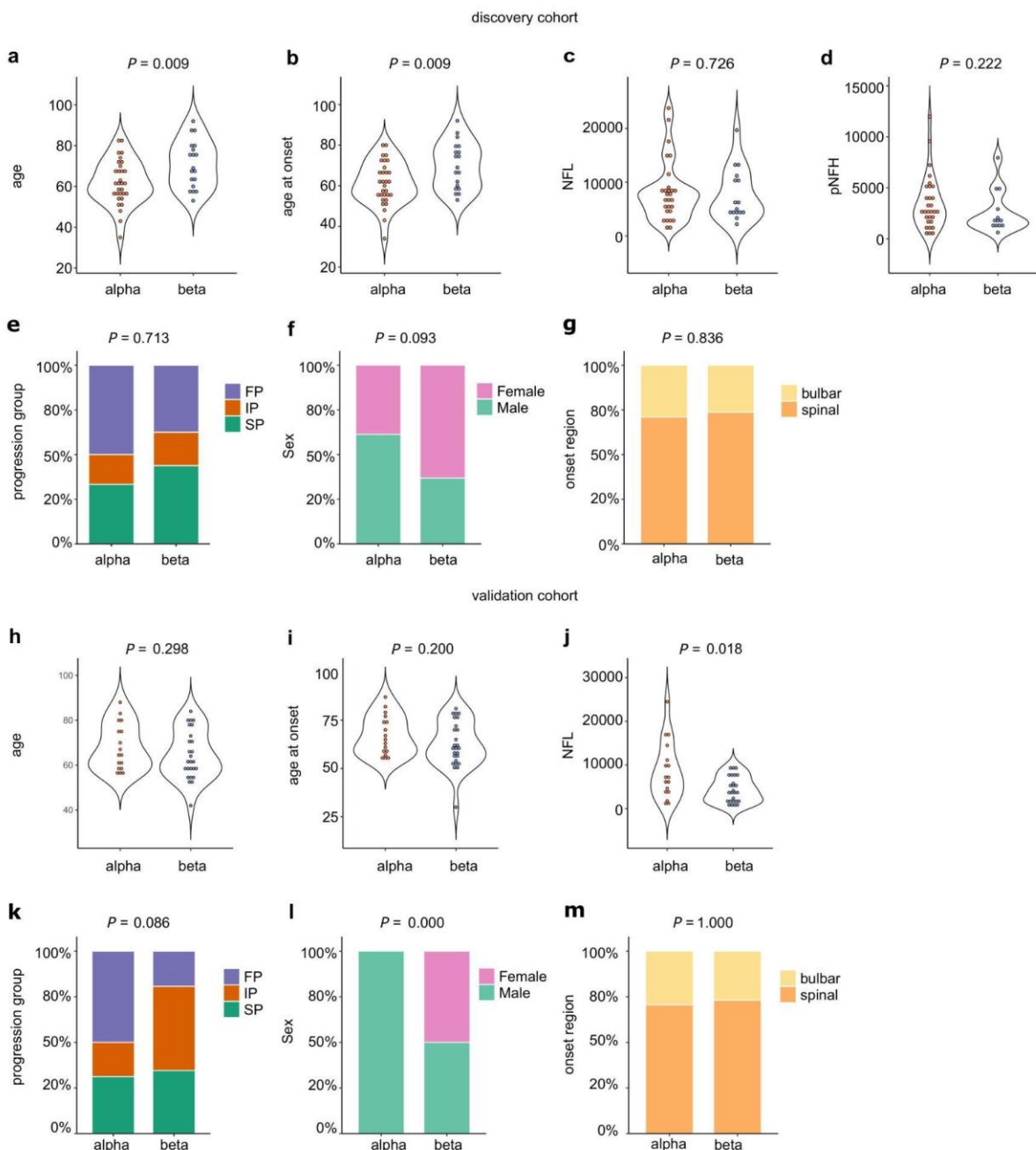
92 **a**, Number of ALS patients assigned to the alpha, beta, or theta cluster in the external cohort
93 (EC; $n = 43$ ALS).

94 **b**, Uniform Manifold Approximation and Projection (UMAP) showing the distribution of
95 proteomic samples using $k = 2$ clustering in the external cohort. Samples are labeled according
96 to assignment to the alpha (orange) or beta (blue) cluster.

97 **c**, Volcano plot of differentially expressed proteins between the alpha and beta clusters in the
98 external cohort. The x-axis shows \log_2 fold change and the y-axis shows $-\log_{10}(\text{FDR})$. Proteins
99 more abundant in the beta cluster are shown in blue and those more abundant in the alpha
100 cluster in orange. Statistical testing was performed using a two-sided test with Benjamini–
101 Hochberg correction for multiple comparisons.

102 **d**, Gene set enrichment analysis (GSEA) of Gene Ontology Biological Process (GO BP) terms
103 identifying the top 20 significantly enriched pathways (FDR < 0.05) distinguishing the alpha
104 and beta clusters in the external cohort. GO BP terms more enriched in the beta cluster are
105 shown in blue, whereas those more enriched in the alpha cluster are shown in orange. Data
106 are represented as signed $-\log_{10}(\text{FDR})$. Related GO terms were manually grouped into
107 broader functional categories.

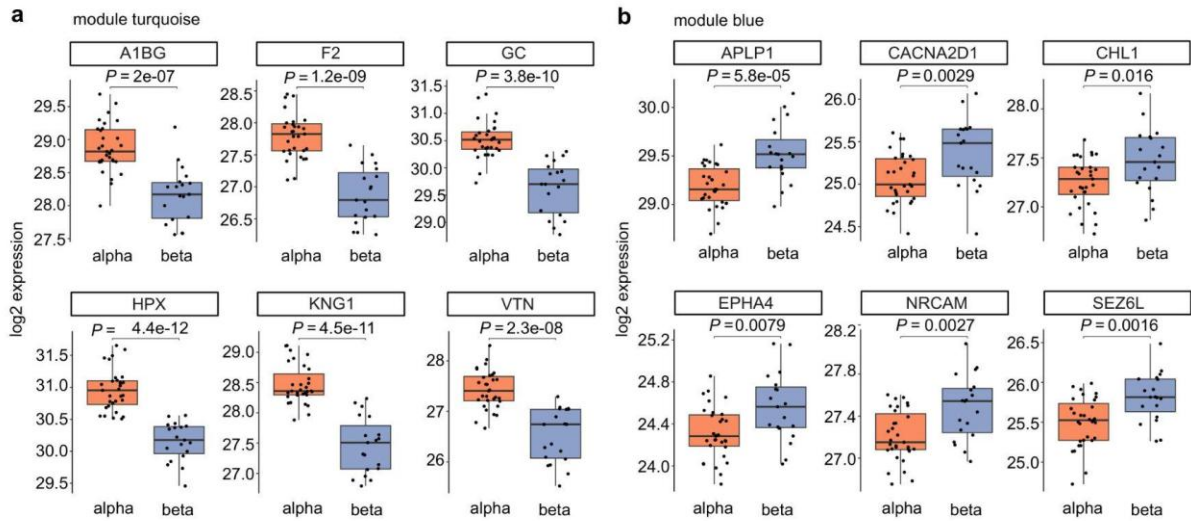
108 **e**, Box plots showing expression levels of ATRN, CNTN1, and PCSK1N in the external cohort.



109

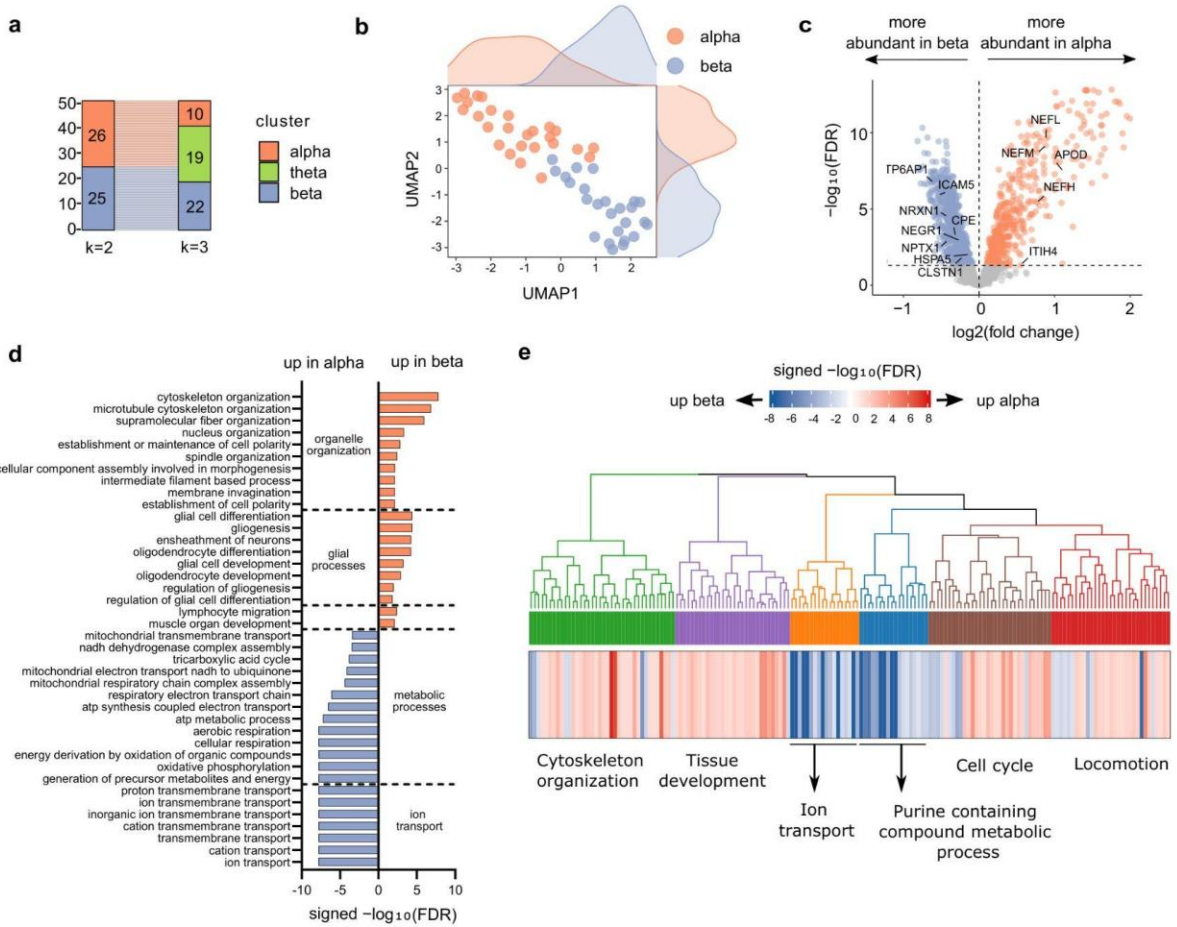
110 **Extended Data Fig. 8 | Clinical characteristics stratified by ALS alpha and beta subtypes**
 111 **in the discovery and validation cohorts.**

112 **a-g**, Clinical characteristics stratified by alpha and beta subtypes in the discovery cohort.
 113 **h-m**, Clinical characteristics stratified by alpha and beta subtypes in the validation cohort.
 114 Shown are mean age (years) (a,h), mean age at onset (years) (b,i), cerebrospinal fluid
 115 neurofilament light chain (NEFL, pg ml⁻¹) (c,j), cerebrospinal fluid phosphorylated
 116 neurofilament heavy chain (pNFH, pg ml⁻¹) (d), disease progression group (e,k), sex (f,l), and
 117 site of onset (g,m). Statistical analyses are described in the Methods. $P < 0.05$ was considered
 118 statistically significant.



120 **Extended Data Fig. 9 | Top 6 proteins of the turquoise and blue modules in the discovery**
 121 **cohort.**

122 **a,b**, Boxplot showing the expression levels of the top 6 proteins in the turquoise **(a)** and the
 123 blue **(b)** module. Each dot represents an individual sample. The box indicates the interquartile
 124 range (IQR), the line within the box represents the median, and the whiskers extend to
 125 $1.5 \times \text{IQR}$. $P < 0.05$ was considered statistically significant.



126

127 **Extended Data Fig. 10 | Clustering of brain proteomic samples.**

128 **a**, Number of ALS patients within the alpha, beta, or theta cluster in the brain proteomic dataset
129 (n = 51 ALS).

130 **b**, UMAP representation of the human brain proteomic samples for k = 2 clustering. Labels
131 indicate samples assigned to the alpha (orange) or beta (blue) cluster.

132 **c**, Volcano plot showing dysregulated proteins between the alpha and beta clusters in the
133 external cohort. X-axis: \log_2 fold change; Y-axis: $-\log_{10}$ (FDR). Proteins significantly more
134 abundant in beta are shown in blue, and those more abundant in alpha in orange. Statistics
135 were calculated using a two-sided test with Benjamini-Hochberg correction. Proteins
136 previously identified in the CSF alpha and beta clusters are labeled.

137 **d**, Gene Set Enrichment Analysis (GSEA) of the top 20 significant Gene Ontology Biological
138 Processes (GO BP; FDR < 0.05) in the alpha and beta clusters of the external cohort. Blue
139 indicates enrichment in beta, orange in alpha. Data are shown as $-\log_{10}$ (FDR). Related GO
140 terms were manually grouped under general categories.

141 **e**, GSEA of GO BP for alpha vs beta comparisons in the discovery, validation and external
142 cohort. Significantly enriched GO BP terms (FDR < 0.05) were grouped based on semantic
143 similarity, consolidating related terms into six categories named after the highest similar term.
144 Data are represented as signed $-\log_{10}(\text{FDR})$, with blue indicating up in alpha and red up in
145 beta.